CO₂ storage in depleted gas reservoirs: A study on the effect of residual gas saturation

Arshad Raza[1], Raoof Gholami[1], Reza Rezaee[2], Chua Han Bing[3], Ramasamy Nagarajan[4], Mohamed Ali Hamid[1]

1-Department of Petroleum Engineering, Curtin University, Malaysia
E-Mail: arshadraza212@gmail.com
2-Department of Petroleum Engineering, Curtin University, Australia
3-Department of Chemical Engineering, Curtin University, Malaysia
4-Department of Applied Geology, Curtin University, Malaysia

Abstract

Depleted gas reservoirs are recognized as the most promising candidate for carbon dioxide storage. Primary gas production followed by injection of carbon dioxide after depletion is the strategy adopted for secondary gas recovery and storage practices. This strategy, however, depends on the injection strategy, reservoir characteristics and operational parameters. There have been many studies to-date discussing critical factors influencing the storage performance in depleted gas reservoirs while little attention was given to the effect of residual gas. In this paper, an attempt was made to highlight the importance of residual gas on the capacity, injectivity, reservoir pressurization, and trapping mechanisms of storage sites through the use of numerical simulation. The results obtained indicated that the storage performance is proportionally linked to the amount of residual gas in the medium and reservoirs with low residual fluids are a better choice for storage purposes. Therefore, it would be wise to perform the secondary recovery before storage in order to have the least amount of residual gas in the medium. Although the results of this study are useful to screen depleted gas reservoirs for the storage purpose, more studies are required to confirm the finding presented in this paper.

Keywords: CO₂ storage, dry gas reservoir, long term reservoir simulation, residual gas saturation.

1. Introduction

Carbon capture and storage (CCS) technology is an effective greenhouse gas mitigating strategy carried out in recent years. To date, deep saline aquifers, active or depleted oil and gas reservoirs, unminable deep coal seams and salt domes have been recognized as the promising sites to implement the CCS [1]. Depleted oil and gas reservoirs are perhaps one of the most promising candidates for storage projects [2-7], due to their characteristics, proven storage integrity, and subsurface conditions [8-10]. These reservoirs have zero or limited operational costs, with a seal to confine liquids or gases for thousands or millions of years. Their properties, such as porosity, permeability, pressure, temperature and the overall storage capacity are known while many of the equipment installed on the surface or underground may be re-used for CO₂ storage. However, a large fraction of natural gas is often left in reservoirs after depletion, which is referred to as the trapped gas [11, 12], including both residual and the unswept gases. As a result, during an Enhanced Gas Recovery (EGR) process, when injected CO₂ is mixed with the remaining gas,

1

the quality of produced gas is reduced significantly [3, 12-15], even though this mixing is not very extensive [16, 17]. On the other hand, CO_2 injection may induce fault reactivation due to the pressure increase associated with injection [18, 19].

Previous studies investigating depleted natural gas reservoirs stated that the success of an EGR practice and CO_2 storage is linked to the injection strategy, reservoir characteristics and operational parameters. For instance, Oldenburg et al. [3] studied EGR and storage by focusing on the physical processes (i.e., reservoir pressurization, CH_4-CO_2 mixing by advection, dispersion, and molecular diffusion, and pressure diffusivity) associated with injections. The results obtained showed that a significant amount of CO_2 can be injected to produce additional natural gases and mixing would be limited because of the high density and viscosity of CO_2 compared to CH_4. Jikich et al. [8] numerically considered the effects of the injection strategy in two scenarios: i) simultaneous CO_2 injection and methane recovery from the very beginning of the project, and ii) primary production of natural gas to the economic limit, followed by injection of carbon dioxide for the secondary gas recovery. They also assessed the effect of operational parameters (i.e., time of primary production, injector length, injection pressure, injection timing, and production well pressure) on EGR and CO_2 storage. They concluded that injection after field abandonments can provide a better recovery than the early stages. Al-Hashami et al. [20] studied the EGR and the storage by considering the effect of mixing, diffusion and solubility in formation water. They showed that CO_2 solubility has a positive impact on the storage and indicated that an incremental gas recovery of 8% can be achieved by CO_2 injection in a reservoir with a primary recovery (natural reservoir energy) factor of 85% under natural depletion [20]. Polak and Grimstad, [21] adopted a numerical approach to evaluate the EGR and CO_2 storage in the Atzbach-Schwanenstadt gas field of Austria. They found a quick breakthrough of CO_2 which could ultimately limits production. They also reported that the reservoir pressure stabilizes after the stoppage of injection and only 10% of injected CO_2 dissolves in immobile reservoir water after 1500 years [21]. Feather and Archer [12] numerically analyzed the EGR and injection for the storage purpose. They took into account well types, permeability, parabolic and slanted reservoir geometry, injection timing, and injection rate in their modeling. It was then found that vertical wells, the presence of dip slope in the reservoir geometry, low permeability, and homogeneity are favorable for a successful EGR. Khan et al. [13] endorsed CO_2 injection along with the methane recovery. According to their simulation, the higher the rate of CO_2 injection, the higher the natural gas recovery would be.

However, there have only been few studies so far emphasizing changes in characteristics of the multiphase flow in depleted gas reservoirs due to residual hydrocarbon saturation. Saeedi and Rezaee [22], for instance, experimentally studied the effect of residual gas saturation on multiphase characteristics of sandstone samples. They concluded that depleted gas reservoirs may offer a low CO_2 injectivity at early stages which would improve over time with further injection [22]. Snippe and Tucker [23] numerically examined storage in depleted gas fields and

saline aquifers. They concluded that lateral migrations of free CO_2 in the structurally open system depends on absolute permeability, residual gas saturation, and mineral surface areas [23]. Raza et al. [24] reviewed and highlighted the negative impact of residual gas saturation on the storage capacity and injectivity in depleted gas reservoirs. They indicated that the reduction in brine mobility, density and viscosity of gas mixtures when it dissolves into the supercritical CO_2 causes the decrease in storage capacity.

To the best of authors knowledge, there have not been any studies so far evaluating the long-term effect of remaining (residual) gas on the storage capacity, injectivity, reservoir pressure and trapping mechanisms. The aim of this paper is to provide an insight into the long-term aspect of injection into depleted dry gas reservoir by considering the effect of the residual gas saturation.

2. Simulation approach

CO_2 storage in a depleted natural gas reservoirs was modeled using Eclipse300^{TM}, a commercial compositional simulator. The GASWAT (i.e., modeling gas phase/aqueous phase) option in the fully implicit formulation of E300 was used to run all simulation models [25, 26]. This option has been used in earlier studies to enhance the natural gas recovery for CO_2 storage purposes [12]. A 3D Cartesian grid was applied to generate an anticline reservoir geometry structure consisting of 5 fluvial sand and shale layers. Each layer has a thickness of 3 meter with a certain level of heterogeneity, which helps to consider the effect of heterogeneity on the multiphase flow behavior of CO_2 [27]. The depth of the formation was set to be 840 m to ensure that supercritical CO_2 can be appeared. The model has an average porosity and permeability of 0.20 and 100 mD, respectively. The X-Y plane has 532 grid blocks in each direction and the regular size of each grid block in x and y directions was 180 m.

A closed outer boundary condition was considered to make the volumetric gas scenario. A total number of six production wells, P1-P6, were considered in the first two layers, approximately 1 km away from the injection well, I1. This injection well was placed in the lower structure grid at the depth of 2386 m (7828ft), as shown in Figure 1.

For the depletion scenario, the initial reservoir pressure and temperature gradient were set to be 2900 psi and 120 °C/km respectively to simulate a dry gas reservoir. Four components were considered as part of the dry gas as given in Table 1. The capillary entry and fracture pressures of the seal were assumed to be 2600 psia and 4500 psia, respectively. The salinity level of the storage formation was assumed to be 20000 ppm. Properties of gas, water and carbon dioxide (i.e., critical pressure, critical temperature, acentric factors and Lohrenz Bray Clark viscosity coefficients) were generated by the PVTi module of Eclipse. For calculation of PVT properties, the Peng-Robinson equation of state (EOS) was applied [28]. This equation was modified by Soreide and Whitson to determine the solubility of CO_2, N_2, and H_2S in water [29]. The solubility of other gases such as methane and ethane were treated by the original Peng Robinson [25]. The EOS was used to define the diffusive flow in terms of vapor molar functions and diffusion function for gas and water components.
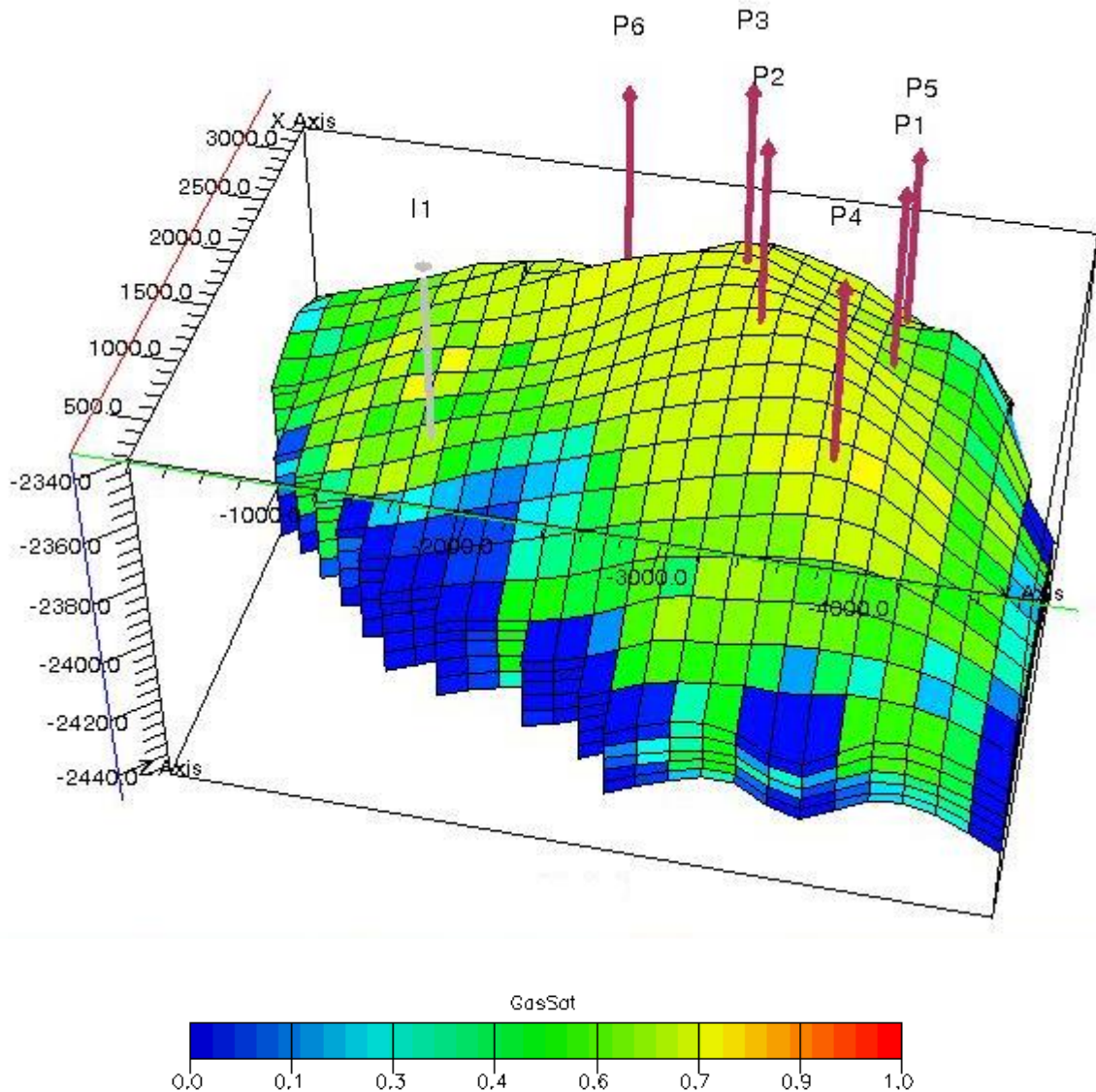
Figure 1: The GASWAT model showing the geometry of the reservoir and locations of all wells. Values on XYZ axis are in metric.

Table 1. Compositions of components at different depths and physical property parameters of five fluvial sand and shale layers

Component	Composition above GWC			
Carbon dioxide (CO_2)	0.002			
Methane (C1)	0.90			
Ethane (C2)	0.08			
Water (H20)	0.018			
Physical property of five fluvial sand and shale layers				
Layers	1, 3,5	2	4	Unit
Porosity	0.01-0.30	0.01-0.17	0.01-0.22	-
Horizontal Permeability	0.1-1000	0.1-200	0.1-500	mD
Vertical Permeability	0.1-500	0.1-50	0.1-100	mD

Relative permeability data for depletion scenario was generated by considering different residual gas saturations for modeling purposes. The residual gas saturation is the lowest saturation at which gas could start to flow. This critical parameter was assumed to be equal to the residual gas saturation, when there was no mobility threshold above this saturation [30, 31]. The relative permeability and the capillary entry pressure curves were generated using the Corey and van Genuchten correlation for gas and water phases [32], using values given in Table 2. The value of parameters given in Table 2 were the same as the ones assumed by Hussain et al. [32] in Table 3. The endpoint relative permeability of 1 was considered at the maximum water and gas saturation of 1 and 0.8, respectively. Table 4 presents the governing equations for the GASWAT modeling.

Table 2: Relative permeability and capillary pressure parameters					
	Residual water saturation (Swr)	Residual gas saturation (Sgr)	Maximum gas relative permeability (Krg_max)	Capillary entry pressure (P$_0$, pisa)	Capillary pressure exponent (λ (λ
Top Seal	0.5	0.2	0.2	2600	0.1
Storage Formation	0.2	0.05 (base case)		1.450	0.3
		0.1	1		
		0.2			
		0.3			

Table 3: Relative permeability and capillary pressure parameters (Hussain et al. [32])					
	Residual water saturation (Swr)	Residual gas saturation (Sgr)	Maximum gas relative permeability (Krg_max)	Capillary entry pressure (P$_0$, pisa)	Capillary pressure exponent (λ)
Top Seal	0.5	0.18	0.35	1740	0.25
Storage Formation	0.2	0.18	0.87	1.450	0.4

Table 4: Governing equation for the GASWAT modeling

Mechanism	Model	Governing Equation
Phase (oil, gas, water) flow [25]	Composition flow	$$F_{pni}^c = T_{ni} y_p^c k_{rp} S_p \frac{b_p^m}{\mu_p} dP_{pni}$$
Fluid Properties [25]	Peng-Robinson EOS	$$\left[P + \frac{A}{V_M (V_M + B) + b(V_M - B)} \right](V_M - B) = RT$$
	Soreide and Whitson modifications	$$\alpha^{\frac{1}{2}} = 1 + 0.4530\left[1 - \left(1 - 0.0103c_s^{1.1}\right)T_r\right] + \left[0.0034(Tr^{-3} - 1)\right]$$ $$k_{jw}^a = bq_1 + bq_2 T_{rj} + bq_3 T_{rj}^2$$

Relative Permeability Corey and van Genuchten correlation [32]	$$k_{rw} = \left(\frac{S_w - S_{wr}}{1 - S_{wr}}\right)^4$$ $$k_{rg} = k_{rg\_max}\left(1 - \frac{S_w - S_{wr}}{1 - S_{wr} - S_{gr}}\right)^2$$ $$P_c = P_0\left(\left(\frac{S_w - S_{wr}}{1 - S_{wr}}\right)^{-\frac{1}{\lambda}-1} - 1\right)^{1-\lambda}$$

According to Jikich et al. [8], injecting CO_2 after the field abandonment is the best scenario for having a better recovery. However, for the purpose of this study, it was assumed that production from the reservoir was started at an optimum production rate and CO_2 injection was then performed for the storage purpose without having any secondary recovery. Flow rates during depletion were selected after a number of simulations to determine the optimum rate for the maximum recovery. The Calorific values of 4.3 BTU/lb.M (10Kj/KgMole) and 8.6 BTU/lb.M (20Kj/KgMole) were assumed for methane and ethane, respectively. Six wells were kept on production for a period of 20 years. At the end of depletion, the initial and remaining gas in place, gas rate, pressure profile, and field gas quality were recorded for four different residual gas saturation cases.

After depletion, different final reservoir pressures were used in the GASWAT storage modeling of the depleted gas scenario. These final pressures in different injection cases develops different levels of remaining gas in terms of field gas in place at the initial stage which was equivalent to the gas volume estimate at the depletion stage. In other words, different levels of remaining gas were developed by utilizing the final depleted pressure. For the multiphase flow in the reservoir, the relative permeability of CH_4-CO_2 and CO_2-H_2O systems were considered for the drainage phenomenon of CO_2 in the depleted gas reservoir for moveable water, as reported by Seo [33].

To highlight depletion, the production wells were shut for 20 years and then pure CO_2 was injected into the storage formation with a bottom hole pressure limit of 2600 psia (equal to the capillary entry pressure of the seal) at different rates for 10 years without recovering the remaining gas. Different layers were then evaluated to achieve the maximum cumulative injection. Various percentages of CO_2, ranging from 57 to 95 % were introduced. After injection, simulation was run for an additional 70 years to observe the long-term changes in the pressure dissipation and trapping mechanisms (i.e., structural, capillary and dissolution) of the reservoir, since the convective mixing may take thousands of years to completely trap the CO_2 plume [34]. The mineral trapping was not evaluated though, due to limitations of the simulator used.

3. Results and Discussion

The simulation was run to evaluate the effect of the residual gas on the key aspects of the storage site such as capacity, injectivity and trapping mechanisms. Before injection, the simulation was done under compositional mode till the depletion stage. During the injection period, an attempt was made to ensure that the pressure build-up does not enhance the seal entry or the fracture pressure in each of these cases. Figure 2 demonstrates the results of the simulation during the production period in terms of total gas in place, pressure, gas rate, and water rate.

From Figure 2 (a), one can conclude that the residual gas saturation develops in a similar way as to that of the field gas in place (FGIP). The direct impact of the residual gas saturation was also observed on the volume of remaining gas in the later stage of production as shown in Figure 2 (b). In fact, it was found that production stabilizes in early years for all cases and starts to decline later depending on the residual gas saturation – early in the case of a high residual gas saturation and vice versa. There was a remarkable fluctuation in the production decline rate which indicates an indirect relationship between the field gas production rate (FGPR) and the residual gas saturation for up to 6 years. However, this relationship becomes direct after these early years until the end of the shut-in period, which could be attributed to the high residual gas saturation and maintenance of the reservoir pressure.
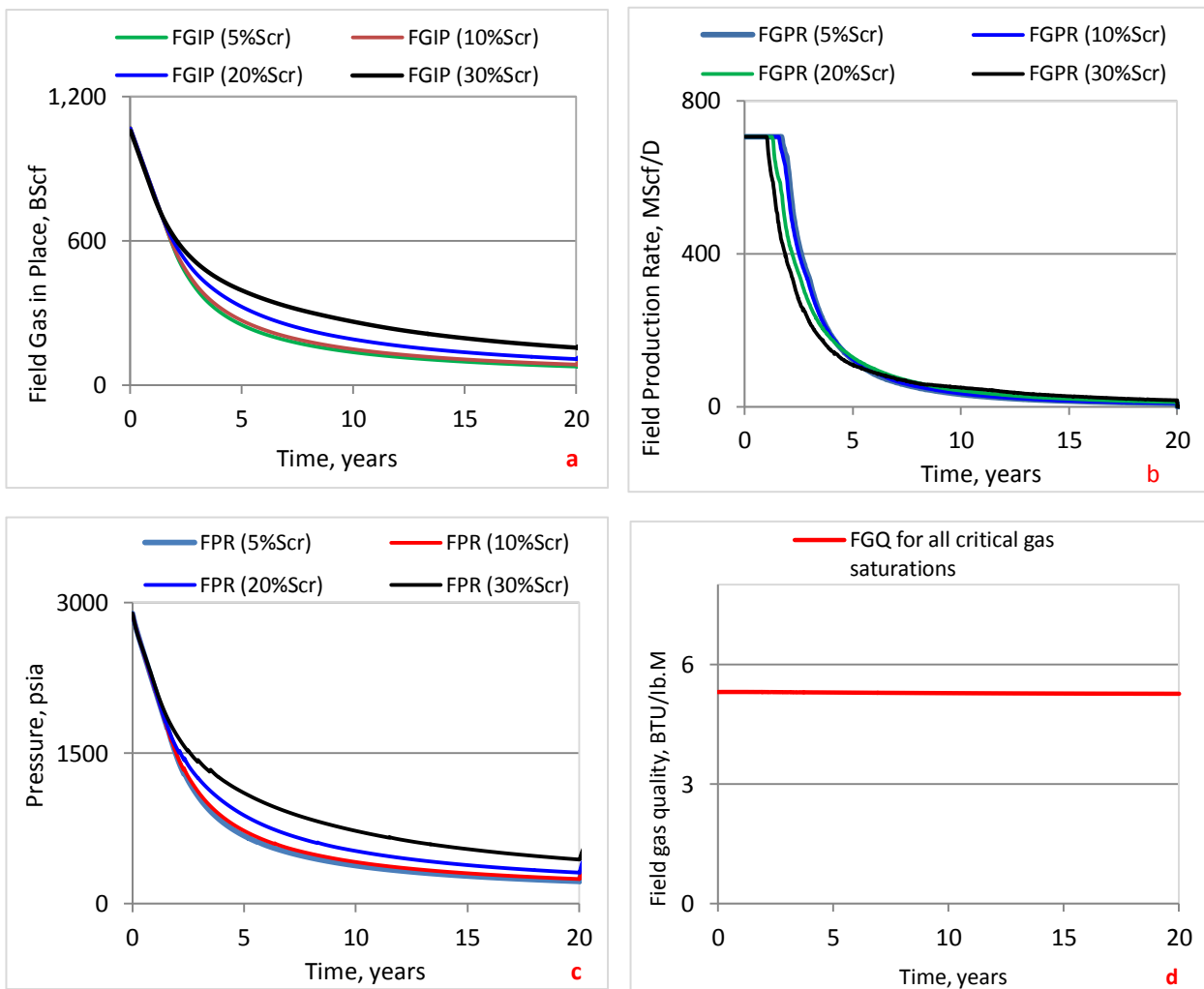
The field reservoir pressure (FPR) decline trend, as shown in Figure 2 (c), depicted that the gas depletion of the close boundary system declines not very fast due to the high compressibility of gas compared to oil and water. The residual gas saturation starts to directly affect the field reservoir pressure in the early stages, which remains and becomes significant till the end of the production period. Therefore, the field reservoir pressure at the stage of depletion is directly related to the residual gas saturation.

During the initial production stage, the field gas quality (FGQ) was stabilized (see Figure 2d) till depletion and no secondary contamination was observed. Therefore, it was noticed that the residual gas saturation may not have any drastic effects on the field gas quality. Figure 2 (e) shows the field water production rates (FWPR) and the total water production (FWPT) before depletion. From this Figure, one can conclude that the production rate stabilizes for a year and it then starts to decline. The total water production at the end of the depletion period of 20 years can be visualized in this figure. Having done this analysis, it was found that the impact of the residual gas saturation on the gas rate would not cause any changes on water extraction. It might be due to the similar relative permeability of water in all cases.

From Figure 3, one can conclude that the amount of the remaining gas at the end of the production period is different for the same GIIP. This is due to consideration of different levels of the residual gas saturation which affects the gas production rate. Therefore, the residual gas saturation is drastically affecting the recovery factor as it controls the relative permeability of gas. Thus, it can be concluded that the residual gas saturation has an indirect relationship with the recovery factor and a direct connection with the volume of the remaining gas at a particular production rate. The ultimate recovery factor (URF) in the considered cases was approximately

80% to 90%, which is mostly offered by the volumetric dry gas reservoir [11]. Figure 4 displays the status of the gas distribution prior to CO_2 injection at the top layer of the storage formation before and after depletion of the dry gas reservoir.

As shown in this Figure, the top view and the cross section of layers are showing the maximum gas saturation of 80% and the remaining gas volume of 78.4 BScf (billion standard cubic feet) after depletion. The remaining gas level in these layers is higher for other cases in which the residual gas saturation was set above 5%. It was observed that a particular quantity of gas has left in all layers after depletion which can be recovered by EGR process. However, it may not be beneficial to recover the remaining natural gas due to the risk of having a mixture of CO_2 and gas. The strategy to inject CO_2 after depletion would help to observe the importance of the remaining gas in the reservoir when it comes to the storage practice.
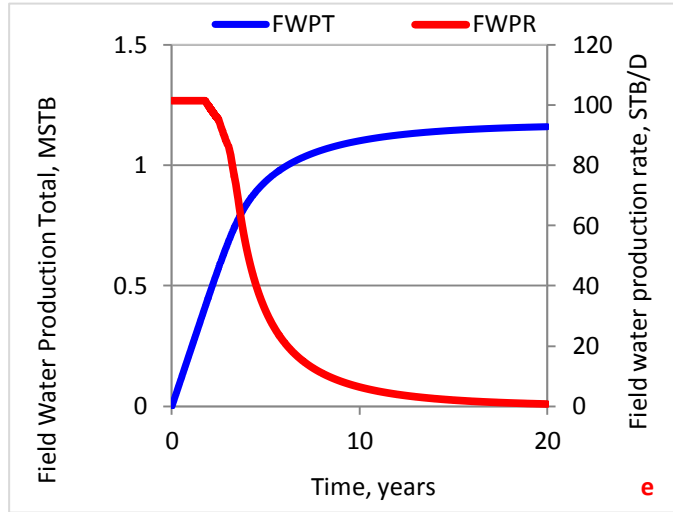
Figure 2. **a:** Field gas in place (FGIP) in four different cases, **b:** Field gas production rate (FGPR) trend in four different cases, **c:** Field reservoir pressure (FPR) against time, **d:** Field gas quality (FGQ) trends in different cases, and, **e:** Field water production rate (FWPR) and field total water production (FWPT)
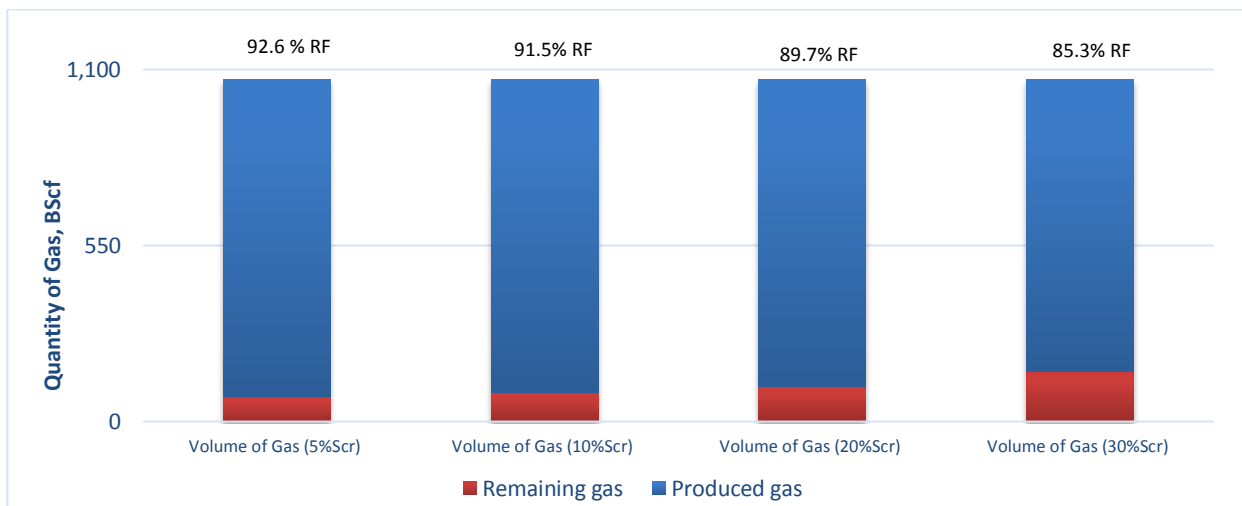

Figure 3. Initial and remaining volumes of gas having various ultimate recovery at different residual gas
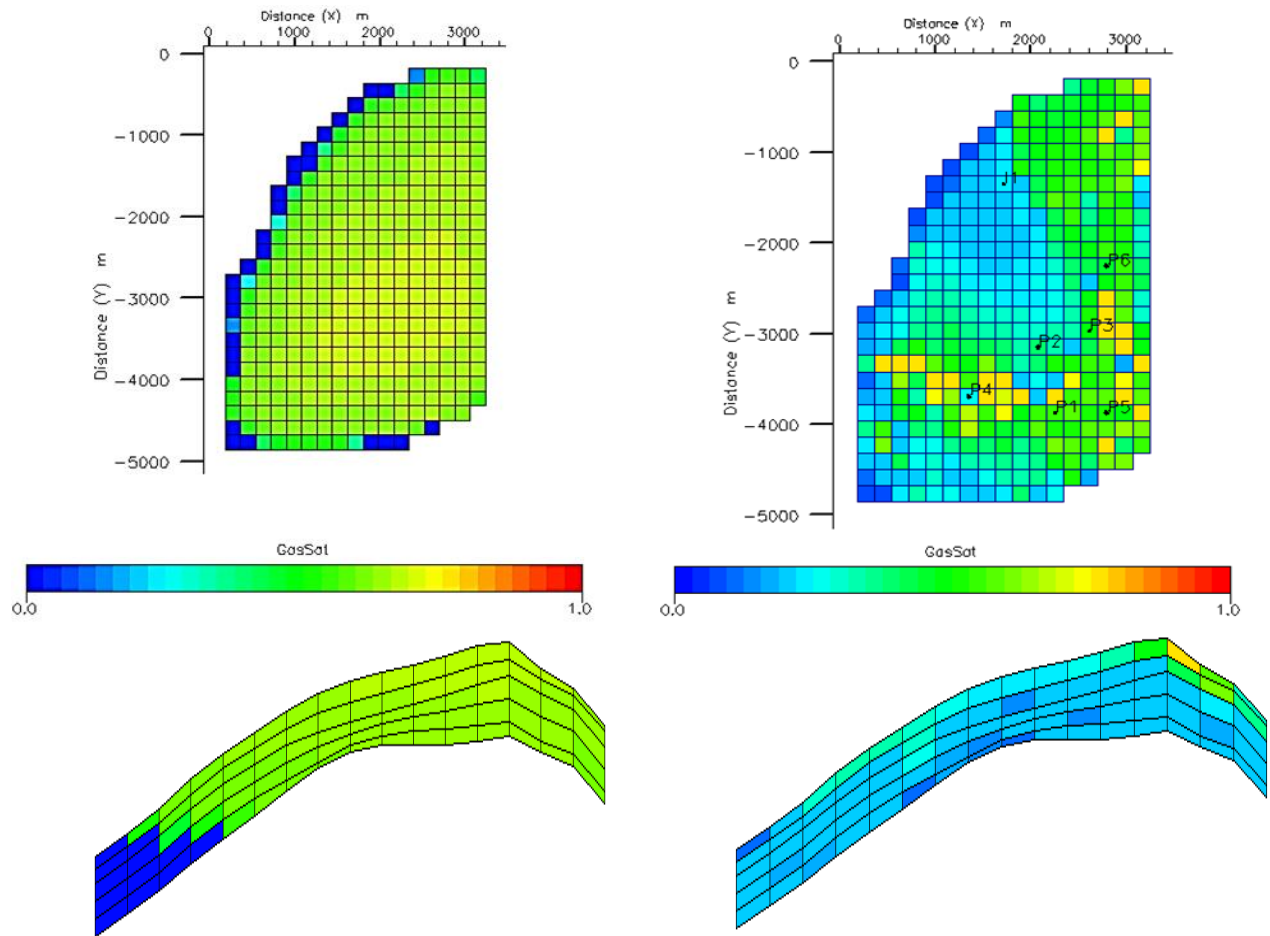
Figure 4. Distribution of gas before (left) and after depletions (right) in the first layer (top view) and all layers (cross section)

Storage capacity, the reservoir volume which can be effectively used for storage purposes, can be estimate using the volumetric method and/or through the production data [35]. This estimation can then be validated by the compositional modeling considering field injectivity and injection constraints [35]. For the purpose of this study, though, the strategy adopted to determine the effective storage capacity is based on the differences between initial gas in place and remaining gas in place at various residual gas saturations. However, based on the simulation results, if the injection pressure is less than the fracture pressure of seal, the volume which can be used for the storage would be equal or less than the effective storage potential as given in Table 5.

After depletion, a comprehensive evaluation covering the whole four cases was conducted to evaluate the potential storage capacity of the site considering different injection rates (i.e., 250 MScf/D, 500 MScf/D, and 700 MScf/D). This analysis was carried out for each and combined zones excluding the location of the injection well. In all cases, the bottom-hole pressure threshold of

2600 psia was used as the injectivity constrain to ensure that the pressure will not exceed the fracture pressure of the caprock. Each zone had different proportions of remaining gas at particular residual gas saturation as summarized in Table 5. Considering the effect of the flow rate on the trapping mechanism, three injection rates were selected to achieve the desired storage potential within ten years of injection. The results obtained also indicated that the cumulative CO_2 injection considering different rates, residual gas saturations, and zones is less than the storage potential, but the left-over storage volume can be approached by further injection for few more years. It is worth mentioning that the quantity of the cumulative CO_2 injected decreases with increasing the remaining gas saturation regardless of zones and injection rates. This might be due to the significant effect of the remaining gas on the injectivity. Taking into account the maximum cumulative CO_2 injected, it seems that zones 1-5 having 15 m thickness are wise choices for injection. In addition, the cumulative CO_2 injected is almost similar for the maximum injections rates of 500 MScf/D (million standard cubic feet per day) and 700 MScf/D which is more than the quantity injected at the maximum injection rate of 250 MScf/D as shown in Figure 5 (a). This is probably due to the similar injectivity behavior at 500 MScf/D and 700 MScf/D which is different than the injectivity at the maximum injection rate of 250 MScf/D. In fact, the behavior of the injection rate in other zones along with their combination is almost similar as observed at 250 MScf/D. It can be seen that sustainability of the injection rate can be achieved with the injection of less than 250 MScf/D, whereas the maximum injection rates of 500 MScf/D and 700 MScf/D are not sustainable from the beginning of the injection. This is because the maximum volume of CO_2 can be injected at the maximum injection rate of 250 MScf/D by increasing the injection period.

Figure 5 (b) shows that injection rates are sustainable from the beginning of injection in zones 1-5, depending on the quantity of remaining gas. It is evident that the remaining gas is drastically affecting the stability of the injection rate and stabilized injection rates are achievable when the quantity of the remaining gas is quite low. By taking into account this relationship, 200MScf/D might be considered as an ideal and accurate optimal injection rate for different residual gas saturations to have a favorable injectivity. However, the injection period must be increased for achieving the desired volume of injected CO_2 if this injection rate is selected.

Table 5: Summary of results obtained from sensitivity analysis on the field injectivity potential

Cases	Injection Rate (MScf/Day) Per field/well	BHP (psia)	Constraints Inj. Period (years)	Zone	Injectivity Issue	Cum. CO$_2$ injected (BScf) Scr = 5% Gas in place = 1068 BScf Remaining gas = 78.4 BScf Storage potential = 990 BScf	Injectivity Issue	Cum. CO$_2$ injected (BScf) Scr = 10% Gas in place = 1068 BScf Remaining gas = 90.4 BScf Storage potential = 977 BScf	Injectivity Issue	Cum. CO$_2$ injected (BScf) Scr = 20% Gas in place = 1068 BScf Remaining gas = 109 BScf Storage potential = 959 BScf	Injectivity Issue	Cum. CO$_2$ injected (BScf) Scr = 30% Gas in place = 1068 BScf Remaining gas = 156 BScf Storage potential = 912 BScf
Case 1	250	2600	10	Zone 1	No	787	No	754	No	658	No	591
				Zone 2	No	789	No	755	No	656	No	592
				Zone 3	No	789	No	755	No	657	No	592
				Zone 4	No	784	No	754	No	655	No	585
				Zone 5	No	783	No	749	No	652	No	587
				Zone 1-2	No	804	No	772	No	670	No	607
				Zone 1-3	No	815	No	776	No	679	No	611
				Zone 1-4	No	818	No	780	No	700	No	612
				Zone 1-5	No	882	No	866	No	818	No	730
				Zone 2-3	No	807	No	772	No	676	No	603
				Zone 2-4	No	808	No	778	No	680	No	613
				Zone 2-5	No	811	No	782	No	669	No	614
				Zone 3-4	No	802	No	769	No	672	No	602
				Zone 3-5	No	807	No	774	No	677	No	607
				Zone 4-5	No	803	No	772	No	667	No	601
Case 2	500	2600	10	Zone 1	No	826	Yes	877	Yes	745	Yes	637
				Zone 2	No	824	Yes	879	Yes	747	Yes	639
				Zone 3	No	821	Yes	876	Yes	743	Yes	633
				Zone 4	No	820	Yes	874	Yes	739	Yes	636
				Zone 5	No	816	Yes	869	Yes	736	Yes	630
				Zone 1-2	No	841	Yes	894	Yes	760	Yes	660
				Zone 1-3	No	848	Yes	896	Yes	766	Yes	661
				Zone 1-4	No	851	Yes	899	Yes	767	Yes	667
				Zone 1-5	No	980	Yes	948	Yes	865	Yes	748
				Zone 2-3	No	841	Yes	805	Yes	760	Yes	655
				Zone 2-4	No	846	Yes	800	Yes	766	Yes	661
				Zone 2-5	No	849	Yes	805	Yes	769	Yes	662
				Zone 3-4	No	836	Yes	790	Yes	758	Yes	652
				Zone 3-5	No	845	Yes	798	Yes	763	Yes	654
				Zone 4-5	No	837	Yes	788	Yes	759	Yes	650
Case 3	700	2600	10	Zone 1	Yes	837	Yes	791	Yes	751	Yes	640
				Zone 2	Yes	839	Yes	789	Yes	750	Yes	640
				Zone 3	Yes	836	Yes	787	Yes	749	Yes	639
				Zone 4	Yes	833	Yes	786	Yes	747	Yes	639
				Zone 5	Yes	831	Yes	782	Yes	744	Yes	637
				Zone 1-2	Yes	856	Yes	809	Yes	773	Yes	660
				Zone 1-3	Yes	861	Yes	815	Yes	779	Yes	665
				Zone 1-4	Yes	866	Yes	816	Yes	782	Yes	670
				Zone 1-5	Yes	985	Yes	951	Yes	867	Yes	775
				Zone 2-3	Yes	853	Yes	807	Yes	770	Yes	659
				Zone 2-4	Yes	859	Yes	812	Yes	759	Yes	669
				Zone 2-5	Yes	863	Yes	816	Yes	780	Yes	656
				Zone 3-4	Yes	852	Yes	805	Yes	765	Yes	654
				Zone 3-5	Yes	857	Yes	808	Yes	772	Yes	659
				Zone 4-5	Yes	851	Yes	804	Yes	769	Yes	660

Figures 5 (c)-(d) plot the trends of FGIR (field gas injection rate) against time at the injections rates of 500 MScf/D and 700 MScf/D, respectively. The selected injection rates are not sustainable and declining just after few years of injection except the injection rate of 500 MScf/D having 92.6% RF at 5% S_{cr}, where the flow rate stabilizes for a few months and then starts to decline. It can also be observed that the high remaining gas quantity is causing difficulty in achieving the rate of 500 MScf/D and 700 MScf/D.
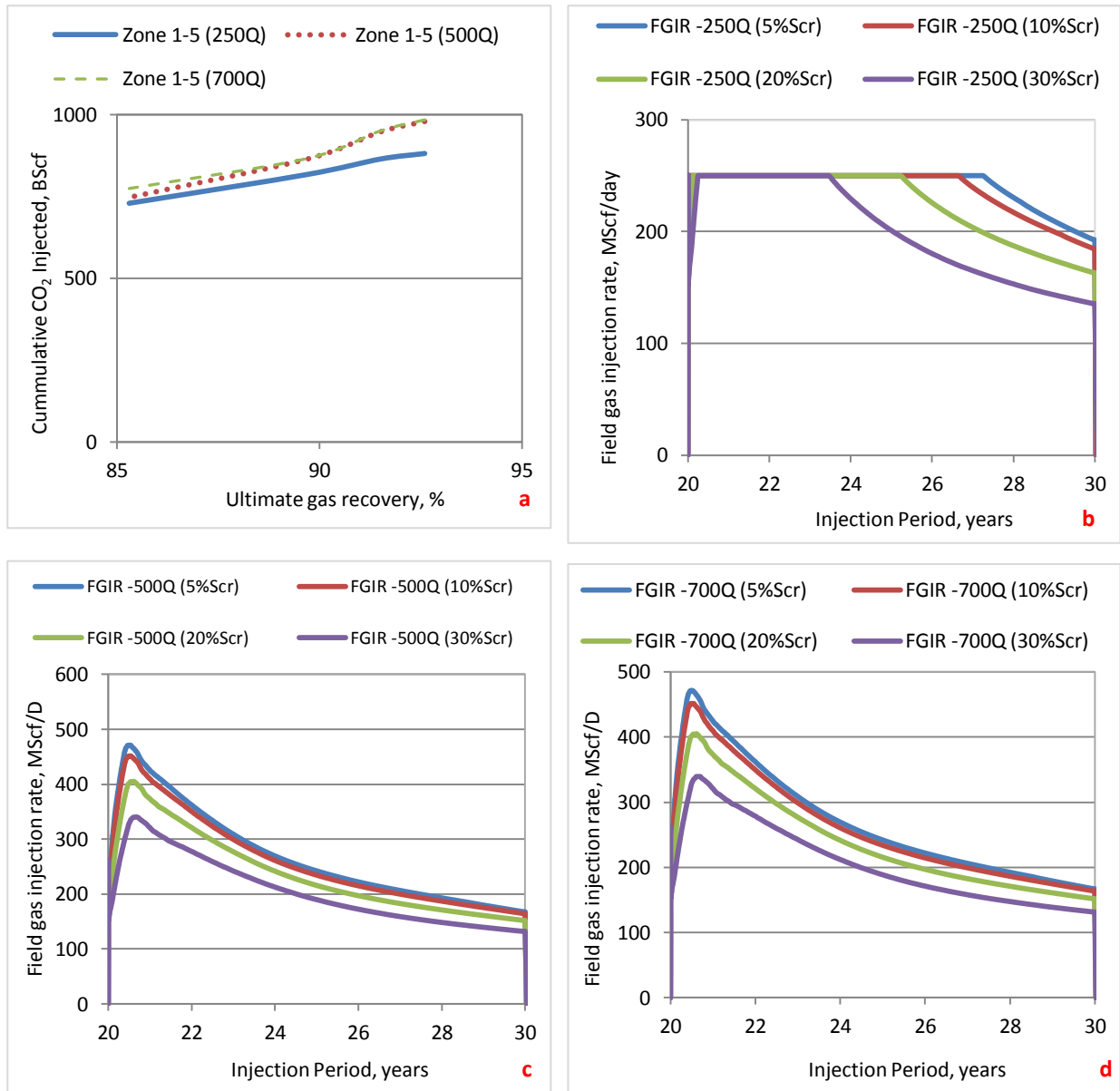
Figure 5. **a** Comparison of cumulative CO_2 injected at different injection rates , **b** Comparison of Injection rate trend at 250 MScf/day considering different level of remaining gas, **c** Comparison of Injection rate trend at 500 MScf/day considering different level of remaining gas, and **d** Comparison of Injection rate trend at 700 MScf/day considering different level of remaining gas

Considering different aspects of storage sites, CO_2 injection would result in pressure buildup, which is controlled by many factors including fluid and rock properties as well as lateral boundary conditions [32]. To evaluate the pressure build-up in all cases described earlier, a closed boundary condition was considered as it does not allow the pressure to dissipate laterally. Based on the profiles shown in Figure 6, the pressure approaches the bottom hole pressure limit while rapid pressure builds up was observed at high injection rates. It was also found that the pressure build-up at the injection rates of 500 MScf/D and 700 MScf/D are similar, which might be due to their injectivity behaviors. The situation could become worse at higher rates with favorable injectivity when pressure may exceed the fracture pressure of the storage formation and seal. The results of simulations for trapping mechanisms at the injection rate of 250 MScf/D were plotted in Figures 7.

As seen in Figure 7 (a), any increase in the residual gas sautration or the volume of remaining gas changes the amount of the structural trapping. It should also be noticed that there is an inverse relationship between the amount of free gas and remainin gas till the end of the injection period. In addition, this relationship remains the same during the observation period of 70 years. As the injected CO_2 flows upward due to buoyancy, free gas and remaining gas may restrict the buoyancy process through which injected CO_2 act as a free gas. This may also be due to the capillary trapping phenomenon after stoppage of injection as shown in Figure 7 (b).

Displayed in Figure 7 (b), the capillary trapping increases linearly during the injection period at a particular saturation. In fact, there is a linear relationship between the residual gas saturation and immobile CO_2 saturation during and after injection. This relationship, however, is remarkable at a high residual gas saturation (20% and 30% S_{cr}). This indicates that presence of remaining gas would be useful to achieve a high capillary trapping, but more studies are still required to confirm this finding. Figure 7 (c) shows that dissolution trapping is inversely related to the residual gas saturation and would be significant at a low level of saturation. However, CO_2 dissolution approximately remains constant after in injection stops and till the end of 100 years, which may start to increase after 100 years during the dissolution of capillary trapped CO_2. Practically, the dissolution trapping increases when the capillary trapped CO_2 starts to dissolve into the brine [32,34, 36], which can be experienced after 100 years. The dissolution rate is controlled by the rate at which dissolved CO_2 is transported away from the interface of CO_2 and brine, which allows fresh brine to reside in close contact with free-phase CO_2. The transport of the dissolved CO_2 can occur by diffusion, advection or and convection [37]. The pressure reduction due to CO_2 dissolution enhanced by the convective mixing is important [38], depending on the pressure and temperature conditions as well as the salinity of brine [39] as seen in Figure 7 (d). After the injection period, the pressure reduction can be attributed to the dissolution and capillary trapping at the high residual gas saturation case.

A comparison was made at the low injection rate of 250 MScf/D among the trapping mechanisms considering different residual gas saturations as shown in Figures 8 (a-d). The results obtained

from such comparison indicated that all trapping mechanisms increase linearly during injection, where structurally trapping is dominant at a low level residual gas saturation (i.e., 5% and 10% S_{cr}). This may increase the risk of losing cap rock integrity due to the long-term exposure to free CO_2 saturation if this situation prevails [40-51]. On the other hand, capillary trapping is dominated more than structural and dissolution trappings at a high residual gas saturation of 30%. In fact, the remaining gas is drastically affecting the structural and dissolution trapping at this level of saturation. It can be concluded that CO_2 mixing with volume resident gas is directly favoring snap-off process to achieve more capillary trapped CO_2 volume.

It worth mentioning that the amount of free gas is increasing slightly during the observation period at residual gas saturations of 5% and 10%, which is probably linked to the decrease in CO_2 dissolution. This increase becomes much more significant at a high residual gas saturation of 20% and 30 % when the capillary trapping increases with the reduction of structural trapping.
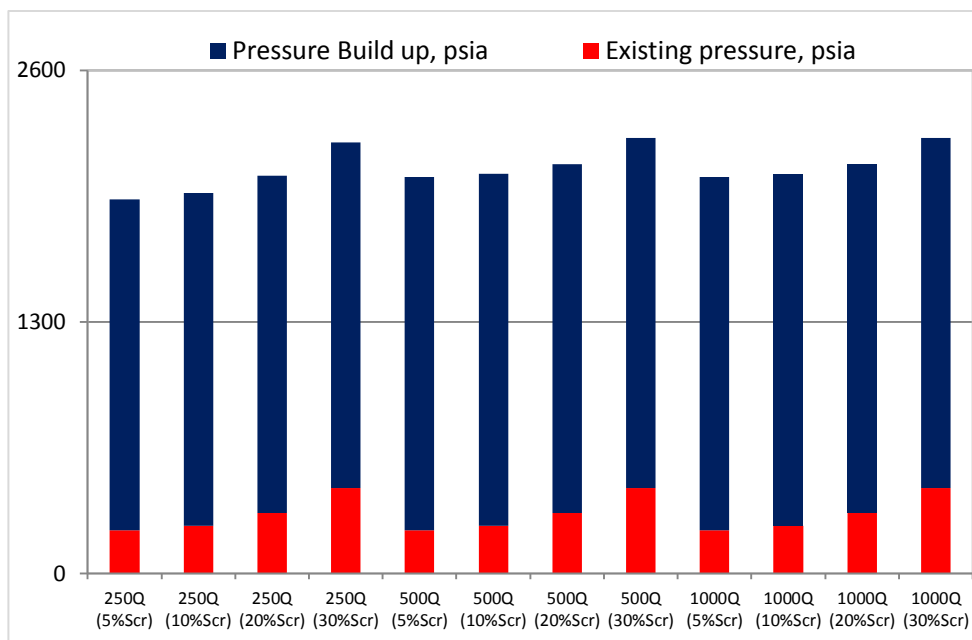

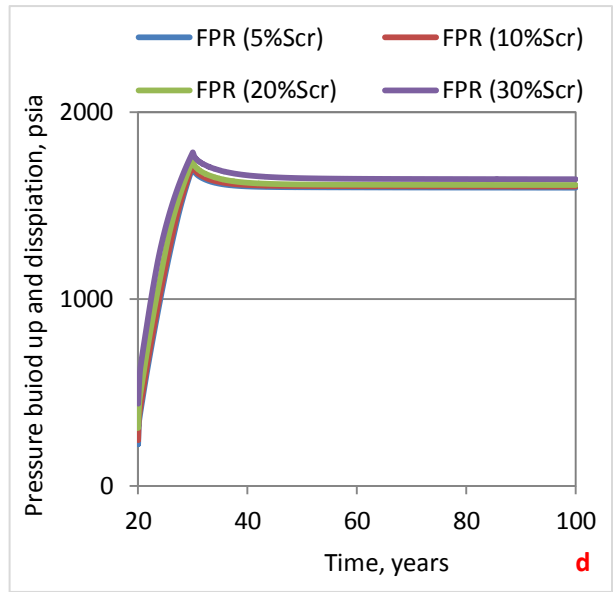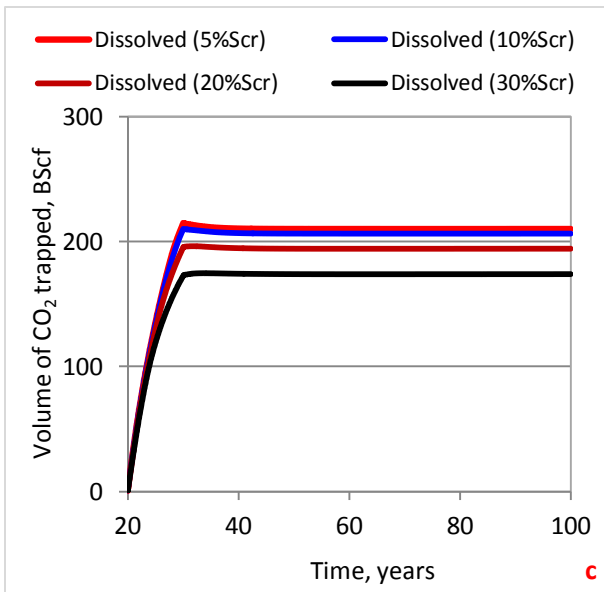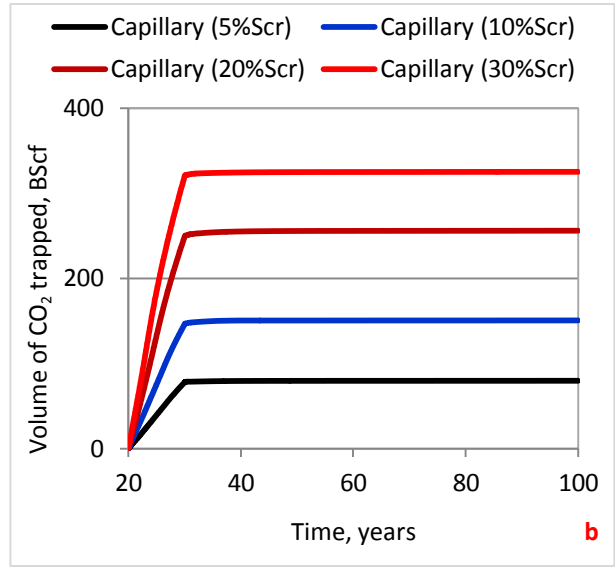Figure 6. Pressure potential at the end of depletion (Red) and injection period (dark blue)
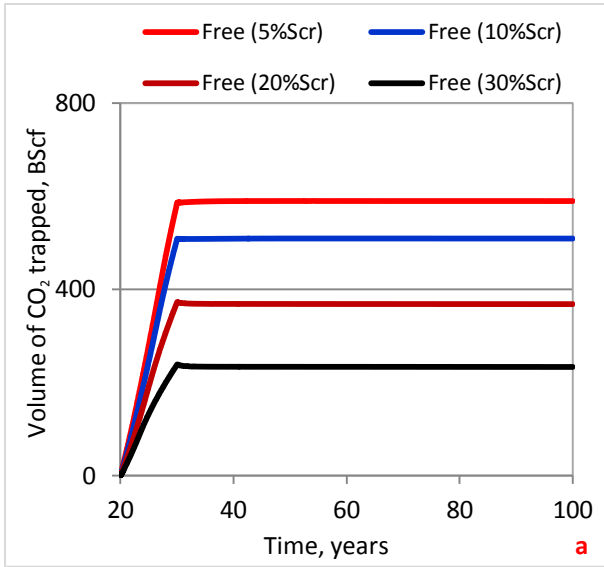
Figure 7. a, Comparison of Free CO_2 at the injection rate of 250 MScf/D, **b** Comparison of capillary trapped CO_2 saturation at the injection rate of 250 MScf/D, **c** Comparison of dissolved CO_2 saturation at the injection rate of 250 MScf/D, and **d** Pressure profile after injection
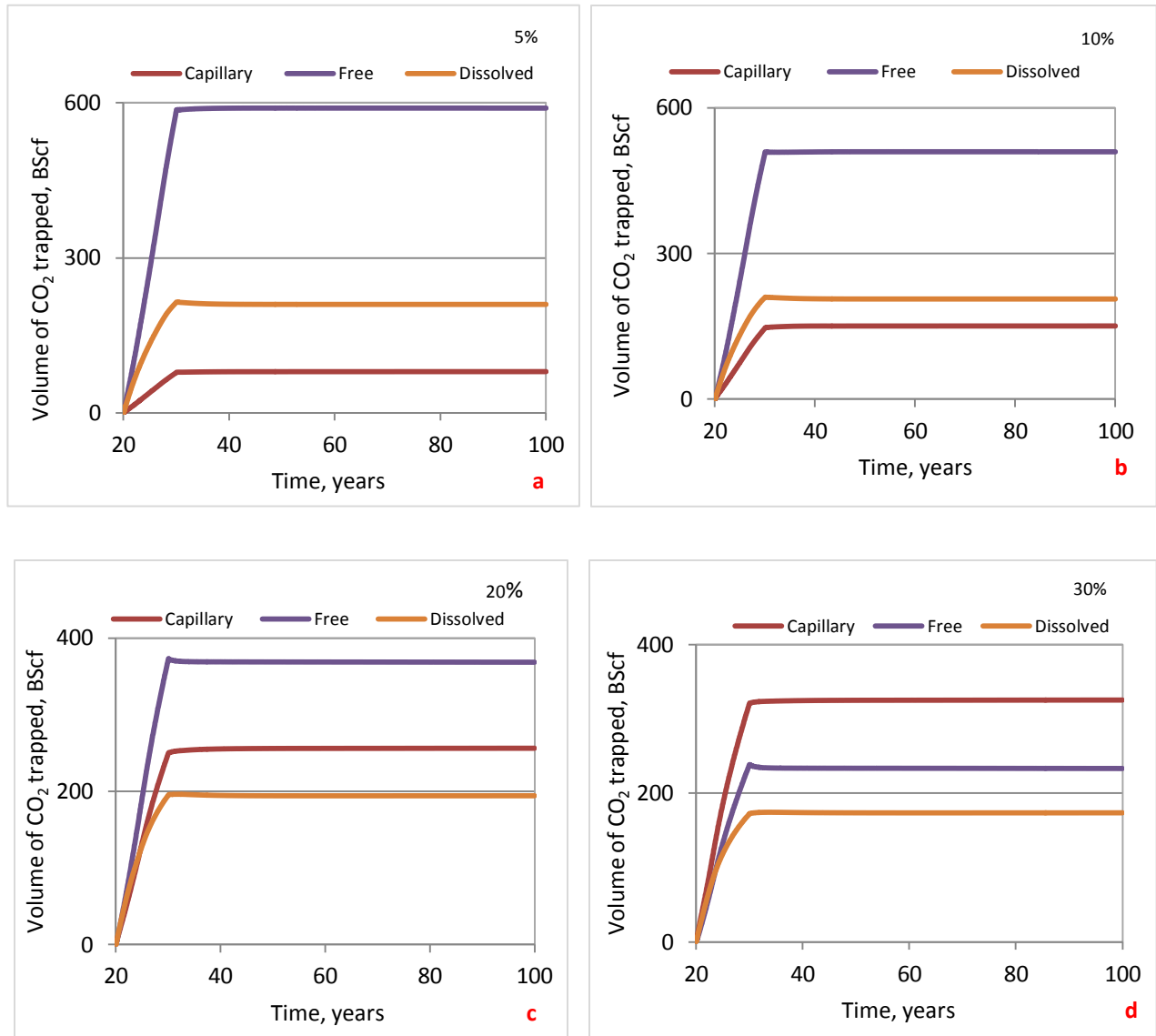
Figure 8. Trapping mechanisms at different residual gas saturations and the injection rate of 250 MScf/D

Table 6 summarizes the results at 250 MScf/D injection rate obtained from comparing different residual gas saturations. A very same analysis was done for other zones in individual and combination ways to evaluate the trend of free, residual and dissolution trapping mechanisms. The results obtained indicated a similar trend against time with differences in the quantity of CO_2 trapped. No major impact was also observed in different zones.

Table 6: Summary of the results obtained from the analysis of Case A (zone 1-5) for the effect of the residual gas saturation on trapping mechanisms

Residual gas saturation	Constraints		Injection rate (MScf/D)	Cumulative CO_2 injected (BScf)	CO_2 Trapped till 100 years, BScf		
	BHP (psia)	Injection time & duration (years)			Free	Capillary	Dissolved
5%	2601	20-30/10 years	250	882	590.6	81.5	209.9
10%	2601	20-30/ 10	250	866	509.2	150.6	206.2
20%	2601	20-30/ 10	250	818	367.8	256.1	194.1
30%	2601	20-30/ 10	250	732	*233.3*	325.4	173.3

Conclusion

In this study, attempts were made to evaluate the effect of the remaining gas on key CO_2 storage aspects of dry gas reservoirs. The results obtained revealed that selection of the storage medium considering the amount of remaining gas is important to achieve a high effective storage capacity with sustainable injection rates. This study also indicated that there is a direct relationship between remaining gas and the capillary trapping, while an inverse correlation exists with the sustainability of injection rate, structural and dissolution trappings and storage capacity. The reservoir with a high amount of remaining gas may offer a high-pressure build up and elevates the security risk. Since the impact of the remaining gas becomes significant on the sustainability of injection rates at high-level injection rates, it would be wise to select a low injection rate for a favorable injectivity when the level of remaining gas in the reservoir is significant.

Acknowledgment

Nomenclature

CCS	Carbon capture and storage
EGR	Enhanced Gas Recovery
CO_2	Carbon dioxide
MPa	Megapascal
CH_4	Methane
m	meters
mD	millidarcy
ft	feet
psia	pounds per square inch absolute
ppm	parts per million
N_2	Nitrogen
H_2S	Hydrogen sulfide
C1	Methane
C2	Ethane
Swr	Residual water saturation

Sgr	Residual gas saturation
Krg_max	Relative gas permeability
P_0	Capillary entry pressure
λ	Capillary pressure exponent
F_{pni}^{c}	Flow rate component in a phase (p=o, w, g), (mol/hour)
T_{ni}	Transmissibility between cells n and i
y_{p}^{c}	Concentration of component c in phase p, (mole fraction)
k_{rp}	Relative permeability of phase
S_p	Saturation of phase p, (fraction)
b_{p}^{m}	Molar density of phase p, (mol/m³)
b_{g}^{m}	Molar density of gas, (mol/m³)
μ_p	Viscosity of phase p, (cp)
T_{ni}	Transmissibility between cells n and i, (cP-rb/day/psi)
dP_{pni}	Potential difference of phase p between cells n and i, (psia)
P	Pressure, (psia)
V_M	Molar volume, (cubic feet/ lb mole)
R	Gas constant, (psia.cu.ft/lb. mole)
A, B	Mixture-specific functions of T and composition with the mixing rules
T	Temperature, (ºF)
T_r	Reduced temperature
C_s	Salinity (ppm or molality)
bq_i	Soreide and Whitson consants
BTU/lb.M	British thermal unit per pound meter
FGIP	Field gas in place
FGPR	Field gas production rate
FPR	Field reservoir pressure
FGQ	Field gas quality
FWPR	Field water production rate
FWPT	Field total water production
URF	Ultimate recovery factor
BScf	Billion standard cubic feet
MScf	Million standard cubic feet
MScf/D	Million standard cubic feet per day
MSTB	Million stock tank barrel
MSTB/D	Million stock tank barrel per day

References

[1].   Bachu, S. Screening and ranking of hydrocarbon reservoirs for CO_2 storage in the Alberta Basin, Canada. in US Department of Energy–National Energy Technology Laboratory, National Conference on Carbon Sequestration. 2001. Pp: 1-11.

[2].   Dance, T., Assessment and geological characterisation of the CO2CRC Otway Project CO_2 storage demonstration site: From prefeasibility to injection. Marine and Petroleum Geology, 2013. 46(0): p. 251-269.

[3].   Oldenburg, C.M. and S.M. Benson, CO_2 injection for enhanced gas production and carbon sequestration. 2001, SPE International Petroleum Conference and Exhibition in Mexico held in Villahermosa, Mexico, 10–12 February 2002.. Society of Petroleum Engineers Inc.: pp. 1-10.

[4].   Pamukcu, Y., Hurter, S., Jammes, L., Vu-Hoang, D., & Pekot, L., Characterizing and predicting short term performance for the In Salah Krechba field CCS joint industry project. Energy Procedia, 2011. 4(0): p. 3371-3378.

[5]. Solomon, S., Carbon dioxide storage: Geological security and environmental issues–Case study on the Sleipner Gas field in Norway. Bellona Report, May, 2007.

[6]. Underschultz, J., Boreham, C., Dance, T., Stalker, L., Freifeld, B., Kirste, D., & Ennis-King, J.., CO_2 storage in a depleted gas field: An overview of the CO2CRC Otway Project and initial results. International Journal of Greenhouse Gas Control, 2011. 5(4): p. 922-932.

[7]. Wright, I.W. The In Salah gas CO_2 storage project. in IPTC 2007: International Petroleum Technology Conference. 2007.

[8]. Jikich, S. A., Smith, D. H., Sams, W. N., & Bromhal, G. S. Enhanced Gas Recovery (EGR) with carbon dioxide sequestration: A simulation study of effects of injection strategy and operational parameters. in SPE Eastern Regional Meeting. 2003. 6-10 September, Pittsburgh, Pennsylvania. Society of Petroleum Engineers: pp. 1-9.

[9]. Raza, A., Gholami, R., Rezaee, R., Bing, C.H., Nagarajan, R. and Hamid, M.A., Preliminary assessment of CO_2 injectivity potential in carbonate storage sites. Petroleum, KeAi, 2016. 3/1: p. 144-154.

[10]. Raza, A., Gholami, R., Rezaee, R., Bing, C.H., Nagarajan, R. and Hamid, M.A., Well selection in depleted oil and gas fields for a safe CO_2 storage practice: a case study from Malaysia. Petroleum, KeAi, 2016. 3/1: p. 167-177.

[11]. Ahmed, T., Reservoir engineering handbook. Gulf Professional Publishing, Elsevier, 2001. 3rd Edition: p. 1-1235.

[12]. Feather, B. and R. Archer. Enhance natural gas recovery by carbon dioxide injection for storage purposes. in In 17th Australia Fluid Mechanics Conference held in Auckland, New Zealand. 2010. pp: 1-6

[13]. Khan, C., R. Amin, and G. Madden, Carbon dioxide injection for enhanced gas recovery and storage (reservoir simulation). Egyptian Journal of Petroleum, 2013. 22(2): p. 225-240.

[14]. Stevens, S., V. Kuuskraa, and J. Taber, Sequestration of CO_2 in depleted oil and gas fields: Barriers to overcome in implementation of CO_2 capture and storage (disused oil and gas fields). Report for the IEA Greenhouse Gas Research and Development Programme (PH3/22), 1999. 87: p. 81A-81.

[15]. Xiaoling, S., Z. Fangui, and L. Hejuan, CO_2-CH_4 system mixing properties and enhanced natural gas recovery. International Journal of Digital Content Technology & its Applications, 2012. 6(21): p. 1-5.

[16]. Oldenburg, C.M., Carbon dioxide as cushion gas for natural gas storage. Energy & Fuels, 2003. 17(1): p. 240-246.

[17]. Van der Meer, B., Carbon dioxide storage in natural gas reservoir. Oil & gas science and technology, 2005. 60(3): p. 527-536.

[18]. Tenthorey, E., Dance, T., Cinar, Y., Ennis-King, J., & Strand, J. Fault modelling and geomechanical integrity associated with the CO2CRC Otway 2C injection experiment. International Journal of Greenhouse Gas Control, 2014. 30: p. 72-85.

[19]. Mildren, S. D., Hillis, R. R., Lyon, P. J., Meyer, J. J., Dewhurst, D. N., & Boult, P. J. , FAST: A new technique for geomechanical assessment of the risk of reactivation-related breach of fault seals. 2005.

[20]. Al-Hasami, A., S. Ren, and B. Tohidi. CO_2 injection for enhanced gas recovery and geo-storage: reservoir simulation and economics. in SPE Europec/EAGE Annual Conference. 2005. 3-16 June, Madrid, Spain Society of Petroleum Engineers. pp: 1-7.

[21]. Polak, S. and A.-A. Grimstad, Reservoir simulation study of CO_2 storage and CO2-EGR in the Atzbach–Schwanenstadt gas field in Austria. Energy procedia, 2009. 1(1): p. 2961-2968.

[22]. Saeedi, A. and R. Rezaee., Effect of residual natural gas saturation on multiphase flow behaviour during CO_2 geo-sequestration in depleted natural gas reservoirs. Journal of Petroleum Science and Engineering, 2012. 82–83(0): p. 17-26.

[23]. Snippe, J. and O. Tucker, CO_2 fate comparison for depleted gas field and dipping saline aquifer. Energy Procedia, 2014. 63(0): p. 5586-5601.

[24]. Raza, A., Rezaee, R., Gholami, R., Bing, C.H., Nagarajan, R. and Hamid, M.A., A screening criterion for selection of suitable CO_2 storage sites. Journal of Natural Gas Science and Engineering, 2016. 28: p. 317-327.

[25]. Schlumberger, Technical Description 2014. 2014.2.

[26]. Schlumberger, Reference Manual. 2014. 2014.2.

[27]. Kuo, C.-W., J.-C. Perrin, and S.M. Benson, Simulation studies of effect of flow rate and small scale heterogeneity on multiphase flow of CO_2 and brine. Energy Procedia, 2011. 4(0): p. 4516-4523.

[28]. McCain, W.D., The properties of petroleum fluids. 2nd edition ed. 1990, Penn Well Books, Penn Well Publishing company, TULSA, Oklahoma, USA. pp: 1-500.: PennWell Books.

[29]. Soreide, I. and C.H. Whitson, Peng-Robinson Predictions for Hydrocarbons, CO_2, N_2, and H_2S with pure water and NaCI brine. Fluid Phase Equilibria, 1992. 77: p. 217-240.

[30]. Guerrero, M.T., Estimation of relative permeability from a dynamic boiling experiment. 1998, Stanford University. Master thesis, pp: 1-174.

[31]. Undeland, E., Residual Gas Mobility in Ormen Lange. 2012, Institutt for petroleumsteknologi og anvendt geofysikk. Master thesis, pp: 1-94.

[32]. Hussain, F., K. Michael, and Y. Cinar, A numerical study of the effect of brine displaced from CO_2 storage in a saline formation on groundwater. Greenhouse Gases: Science and Technology, 2015. 6(1): p. 94-211.

[33]. SEO, J.G., Experimental and simulation studies of sequestration of supercritical carbon dioxide in depleted gas reservoirs. 2004, Texas A&M University USA. p. 1-132.

[34]. Elenius, M.T., D.V. Voskov, and H.A. Tchelepi, Interactions between gravity currents and convective dissolution. Advances in Water Resources, 2015. 83: p. 77-88.

[35]. Jalil, M., Masoudi, R., Darman, N. B., & Othman, M., Study of the CO_2 injection storage and sequestration in depleted M4 carbonate gas condensate reservoir Malaysia. 2012. Carbon Management Technology Conference, 7-9 February, Orlando, Florida, USA. pp: 1-14.

[36]. IPCC, IPCC special report on carbon dioxide capture and storage. Prepared by Working Group III of the Intergovernmental Panel on Climate Change, ed. B. Metz, et al. 2005, Cambridge, United Kingdom and New York, NY, USA.pp: 1-500.

[37]. Emami-Meybodi, H., Hassanzadeh, H., Green, C. P., & Ennis-King, J. (2015). Convective dissolution of CO_2 in saline aquifers: Progress in modeling and experiments. *International Journal of Greenhouse Gas Control, Special Issue commemorating the 10th year anniversary of the publication of the Intergovernmental Panel on Climate Change Special Report on CO2 Capture and Storage*, 238–266. doi:http://dx.doi.org/10.1016/j.ijggc.2015.04.003

[38]. Peters, E., Egberts, P., Loeve, D., & Hofstee, C. (2015). CO_2 dissolution and its impact on reservoir pressure behavior. *International Journal of Greenhouse Gas Control, 43*, 115-123.

[39]. Saeedi, A., Experimental study of multiphase flow in porous media during CO_2 geo-sequestration processes, in Springer PhD theses 2012, Springer Science & Business Media: Springer-Verlag Berlin Heidelberg.pp: 1-100

[40]. Berthe, G., Savoye, S., Wittebroodt, C., & Michelot, J. L. (2011). Changes in containment properties of claystone caprocks induced by dissolved CO_2 seepage. *Energy Procedia, 4*, 5314-5319. doi:http://dx.doi.org/10.1016/j.egypro.2011.02.512.

[41]. Bildstein, O., Jullien, M., Crédoz, A., & Garnier, J. (2009). Integrated modeling and experimental approach for caprock integrity, risk analysis, and long term safety assessment. *Energy Procedia, 1*(1), 3237-3244. doi:http://dx.doi.org/10.1016/j.egypro.2009.02.108.

[42]. Chiquet, P., Broseta, D., & Thibeau, S. (2007). Wettability alteration of caprock minerals by carbon dioxide. *Geofluids, 7*(2), 112-122.

[43]. Hangx, S. J. T., Pluymakers, A. M. H., Ten Hove, A., & Spiers, C. J. (2014). The effects of lateral variations in rock composition and texture on anhydrite caprock integrity of CO2 storage systems. *International Journal of Rock Mechanics and Mining Sciences, 69*, 80-92. doi:http://dx.doi.org/10.1016/j.ijrmms.2014.03.001

[44]. Kaldi, J., Daniel, R., Tenthorey, E., Michael, K., Schacht, U., Nicol, A., . . . Backe, G. (2013). Containment of CO_2 in CCS: Role of caprocks and faults. *Energy Procedia, 37*(0), 5403-5410. doi:http://dx.doi.org/10.1016/j.egypro.2013.06.458.

[45]. Li, Z., Dong, M., Li, S., & Huang, S. (2006). CO_2 sequestration in depleted oil and gas reservoirs—caprock characterization and storage capacity. *Energy Conversion and Management, 47*(11–12), 1372-1382. doi:http://dx.doi.org/10.1016/j.enconman.2005.08.023.

[46]. Tian, H., Xu, T., Li, Y., Yang, Z., & Wang, F. (2015). Evolution of sealing efficiency for CO_2 geological storage due to mineral alteration within a hydrogeologically heterogeneous caprock. *Applied Geochemistry, 63*, 380-397. doi:http://dx.doi.org/10.1016/j.apgeochem.2015.10.002.

[47]. Raza, A., Gholami, R., Sarmadivaleh, M., Tarom, N., Rezaee, R., Bing, C. H., Elochukwu, H. (2016). Integrity analysis of CO_2 storage sites concerning geochemical-geomechanical interactions in saline aquifers. *Journal of Natural Gas Science and Engineering, 36PA*, pp. 224-240.

[48]. Garrido, D.R.R., Lafortune, S., Souli, H. and Dubujet, P., 2013. Impact of supercritical CO_2/Water interaction on the caprock nanoporous structure. Procedia Earth and Planetary Science, 7(0): 738-741.

[49]. Karimnezhad, M., Jalalifar, H. and Kamari, M., 2014. Investigation of caprock integrity for CO_2 sequestration in an oil reservoir using a numerical method. Journal of Natural Gas Science and Engineering, 21: 1127-1137.

[50]. Liu, F., Lu, P., Griffith, C., Hedges, S.W., Soong, Y., Hellevang, H. and Zhu, C., 2012. CO_2–brine–caprock interaction: Reactivity experiments on Eau Claire shale and a review of relevant literature. International Journal of Greenhouse Gas Control, 7(0): 153-167.

[51]. Shukla, R., Ranjith, P., Haque, A. and Choi, X., 2010. A review of studies on CO_2 sequestration and caprock integrity. Fuel, 89(10): 2651-2664.